Characterization of Flexible Polyurethane Foams based on Soybean-Based Polyols

Sudipto Das,[1] Mahendra Dave,[2] G. L. Wilkes[1]

[1]*Department of Chemical Engineering, Virginia Tech, Blacksburg, Virginia 24061-0211*
[2]*BioBased Technologies, 1315 N 13th Street, Rogers, Arkansas 72756*

Received 29 January 2008; accepted 2 June 2008
DOI 10.1002/app.29402
Published online 29 December 2008 in Wiley InterScience (www.interscience.wiley.com).

ABSTRACT: Two series of flexible polyurethane foams were fabricated by substituting conventional petroleum-based polyols with increasing amounts of soy-based polyols (SBP) having different hydroxyl numbers. The mechanical properties of the foams were characterized by stress–strain analysis in the compression mode and DMA in tension mode, the cellular morphology was analyzed by SEM and the microphase-separation of the foams was noted by SAXS. Our results showed that the cellular morphology and mechanical properties of the flexible foams were affected significantly by the foam fabrication method and SBP hydroxyl numbers. © 2008 Wiley Periodicals, Inc. J Appl Polym Sci 112: 299–308, 2009

Key words: polyurethane; renewable resources; microstructure; morphology; mechanical properties

INTRODUCTION

Polyurethane (PU) flexible foams were first synthesized by Bayer[1] on a laboratory-scale in 1941. The process was commercialized in 1954 and since then it has been used in various applications such as for cushioning in furniture, mattresses, automobiles, and even clothing.[2] In 1995, PU flexible foams occupied the fifth position in production volume among various plastics and its use continues to grow at a rapid pace throughout the world.[3] The basic formulation used in the manufacture of PU foams includes a polyol, polyfunctional isocyanate, catalysts, blowing agent, and surfactants. Typically, the laboratory-scale synthesis of PU foams involves two steps. In the first step, the polyol (functionality > 2), blowing agent and surfactants are mixed together to form an unreactive premix. The second step involves the addition of the catalyst and isocyanate (functionality ≥ 2) to the premix with very rapid agitation. This initiates the simultaneous polymerization and foaming reactions, both of which are considerably exothermic in nature. The network structure of typical PU foam contains both chemical and physical crosslinks. Although the chemical crosslinks arise due to reaction between isocyanate and polyol hydroxyl groups, the physical crosslinks arise from the microphase separated hard domains because of intermolecular, bidentate hydrogen-bonding between urea moieties (formed from the reaction of the isocyanate groups with water) (Scheme 1). The use of small angle X-ray scattering (SAXS) has been used to establish the presence of a microphase domain morphology in many PU foams.[4–8] The chemical crosslinks arise from the reaction of the hydroxyl groups of the bifunctional or multifunctional polyols and diol higher functionality isocyanate to form urethane linkages that links the urea moieties to the soft segments. Both of these two types of crosslinks play an important role on the final structure, morphology, and mechanical properties of the foams.[9–14] Some of the physical and mechanical properties which are particularly important for the application of flexible foams are their compression–strain behavior including set and recovery (analyzed by indentation force deflection tests, IFD), glass transition (analyzed by dynamic mechanical analysis, DMA), cellular morphology, air flow characteristics, etc.

One of the major ingredients in a flexible foam recipe is the polyol, which traditionally, are derived from petrochemical resources. But decreasing oil resources, fluctuation in oil prices, and the desire to incorporate environmentally friendly renewable materials in the plastics industry have spurred research which focuses on replacing all or part of the petroleum-based polyols (PBP) with those obtained from renewable resources e.g., vegetable oil. Polyols based on various vegetable oils e.g., castor oil, corn oil, palm oil, linseed oil, safflower oil, and rapeseed oil have been used in the past to prepare PU foams.[15–18] Recently, considerable research

Correspondence to: G. L. Wilkes (gwilkes@vt.edu).
Contract grant sponsor: United Soybean Board (USB).

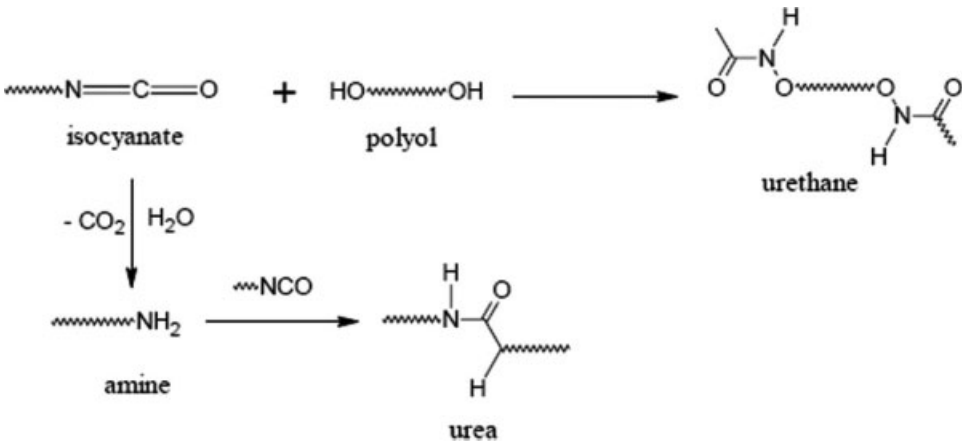

Scheme 1 Chemistry of urethane foam formation.

efforts have been focused on the development of PU's from polyols based on soybean oil because the latter is relatively inexpensive, readily available (it is one of the major crops in North and South America) and research has shown that soybean oil containing PU's may have quite comparable thermal-, oxidative-, and weather-stability relative to PUs comprised solely of PBP-based PU's.[19]

Crude soybean oil contains ca. 95–97% triglycerides, which in turn contains both saturated and unsaturated (ca. 80%) fatty acid residues.[20,21] The three most predominant unsaturated fatty acids in soybean oil are linoleic acid (ca. 53%), oleic acid (ca. 16%), and linolenic acid (ca. 7%) (Fig. 1), but the exact composition of the crude oil is found to vary and depend on factors such as climatic conditions, harvesting condition, soil type, etc.[21–23] Most crude soybean oil of American origin contains ca. 4.6 double bonds per molecule which are unevenly distributed in the various branches of the triglyceride molecule.[21,24] Apart from the unsaturations, the crude oil also contains active sites such as allylic carbons, esters, and α-carbons attached to ester groups,

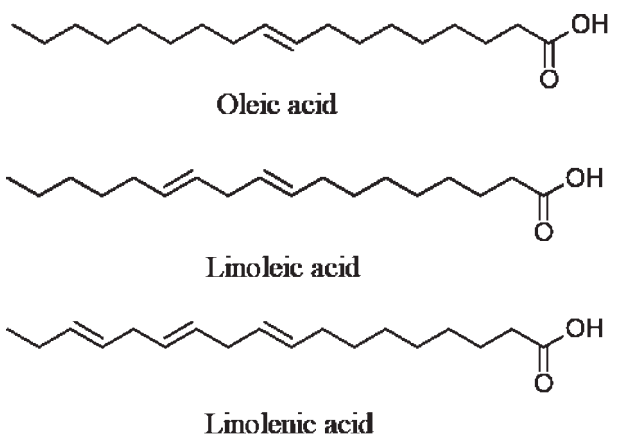

Figure 1 Predominant fatty acids in Soybean oil.

which can be converted to chemical groups such as epoxides,[25] hydroxyls,[26] and aldehydes.[21,22,27,28]

Gou et al.[28] have successfully synthesized soybean-based polyols containing specifically primary (by hydroformylation of soybean oil followed by hydrogenation) or secondary (by epoxidation of the soybean oil followed by methanolysis) hydroxyl groups. John et al.[22] showed that crude soybean oil upon hydroxyl functionalization showed a higher hydroxyl number (OH#), acid value, molecular weight along with lower iodine number, and unsaturated fatty acid content (specifically linolenic acid) than its unmodified counterpart. They successfully prepared flexible PU foams based on soybean-based polyols [SBP, obtained from Urethane Soy Systems Company (USSC), Illinois] using toluene diisocyanate (TDI) or a modified diphenylmethane diisocyanate (MDI). Results showed that although MDI-based foams were more rigid relative to corresponding foams based on TDI as expected, the foaming reaction was faster with TDI. They also probed the foam morphology by use of SEM. Results showed that increased water content in the formulation led to less dense foams with relatively more uniform cell structures. Incorporation of SBP in the foam formulation led to larger and more nonuniform cells.

Singh and Bhattacharya[29] monitored the modulus development during PU foam formation with SBP (obtained from USSC, OH# = 44.25, functionality (f_0) = 2.8) by the use of vane geometry in a strain-controlled rheometer. They identified four stages in the development of modulus during foam formation i.e., (I) bubble nucleation and growth, (II) network packing, (III) microphase separation and cell opening, and (IV) final curing. The flexible foams were synthesized with a blend of PBP (VORNOL obtained from DOW Chemical company, OH# = 56.5, f_0 = 3.0) and SBP and their results showed that increasing the amount of PBP in the formulation led to a significant reduction in reaction time. This

phenomenon was attributed to the presence of "primary" hydroxyl groups in the PBP, which are significantly more reactive than the "secondary" hydroxyl groups in the SBP. They also synthesized two SBP's by ozonolysis of soybean oil (which introduced secondary OH groups, OH# = 64 and 78, $f_0 = 2.3$ and 2.8, respectively). The use of ozonized soybean oil was also found to lead to faster urea microphase separation and decreased overall reaction time (based on rheological analysis) than other SBPs (i.e., obtained from USSC), because of higher hydroxyl number in the former. Further, scanning electron microscopic (SEM) analysis showed that in their SBP-based foams, a coarser texture and more closed cell structures were produced relative to PBP foams.

Mielewski et al.[30] fabricated flexible PU foams containing various amounts of SBP's of an unknown source with MDI and showed that foams containing 40 and 60 wt % SBP's had comparable density, compression-set, tensile strength, and tear-resistance to completely PBP-based flexible foams. Herrington and Malsam[31] synthesized flexible foams by substituting 30% of the total polyol with SBP, which were shown to possess high-load bearing properties without any odor or density changes. More recently, Zhang et al.[32] studied the foam morphology of flexible PU foams prepared by replacing PBP with a SBP (which was functionalized by epoxidation followed by oxirane ring-opening reaction). Their results showed the presence of a higher T_g SBP-rich phase, higher hard segment ordering and enhanced hard domain ordering in SBP-based foams, which in turn improved the compressive modulus of the foams compared to solely PBP-based foams.

This main objective of the work reported here is to probe some of the effects of the systematic replacement of PBP's with various SBP's on the morphology and mechanical properties of the PU foams. Two different flexible PU foam series were fabricated. The first series (Series A) was synthesized in a large wooden box (22″ × 22″ × 42″) by systematic replacement of the PBP (ARCOL F3022 from Bayer) with a SBP (Agrol-A with an OH# 114). The second foam series (Series B) was synthesized in 1000 mL popcorn cups (length = 145 mm, lower diameter = 85 mm, upper diameter = 105 mm), using a different PBP (VORNOL 3136 from DOW Chemical Company) and a different SBP (Agrol-B with an OH# of 140). Although the properties of the SBP were changed in the two series, the two PBP's used in this study (though obtained from different sources) were similar to each other (detailed properties of the various polyols used in this study are described in Table I). The effect of the polyol OH# and foam fabrication process on the cellular morphology (by FESEM), presence of microphase separation of the urea hard domains from the incompatible soft matrix (by SAXS), thermal transitional behavior (by DMA), overall durability (by performing compressive mechanical hysteresis tests), and firmness by indentation force deflection (IFD) measurements of the flexible PU foams were determined in this study and will be reported.

TABLE I
Properties of Various Polyols Utilized in Fabricating Flexible PU Foams

Properties	ARCOL F-3022 (PBP)	VORNOL 3136 (PBP)	Agrol-A (SBP)	Agrol-B (SBP)
Molecular weight, M_n	3000	3100	1750	1918
Hydroxyl number, #OH	56	54	114	140
Polydispersity	–	–	1.17	1.18

EXPERIMENTAL

Materials

As briefly mentioned earlier, the first foam series formulation that was prepared in a large wooden box contained the following ingredients: PBP (ARCOL F3022, obtained from Bayer), SBP (Agrol-A obtained from BioBased Technology (BBT)), surfactant (L-620, obtained from GE Silicone), catalysts (D-19 and C-183, both obtained from GE Silicone), and TDI (80/20 isomer mixture, obtained from Bayer). The second foam formulations which were synthesized in 1000 mL plastic foam cups contained the following ingredients: PBP (VORNOL 3136, obtained from DOW Chemical Company), SBP (Agrol-B obtained from BBT), surfactant (DABCO DC198, obtained from Air Products), catalysts (DABCO BL33LVand DABCO T12, both obtained from Air Products), and TDI was obtained from Aldrich Chemical Company. All the materials were used as received.

Hydroxylation of soybean oil

The functionalization of the soybean oils were conducted at BBT. Refined, bleached, and deodorized soybean oil was oxidized to convert the unsaturation sites present in the triglycerides to hydroxyl and acetate groups[33] (see Scheme 2). The first step involved in situ formation of peracetic acid, which in the second step reacts with the triglyceride double bonds to form an epoxide. In the third step, the epoxide ring is opened to form hydroxyl and acetate groups by acid catalysis. Solvent and impurities are removed at high temperatures and under vacuum.

Preparation of flexible foams

Foams based on Agrol-A SBP (Series A)

The foam components were mixed in a five gallon mixing pail under ambient conditions. The

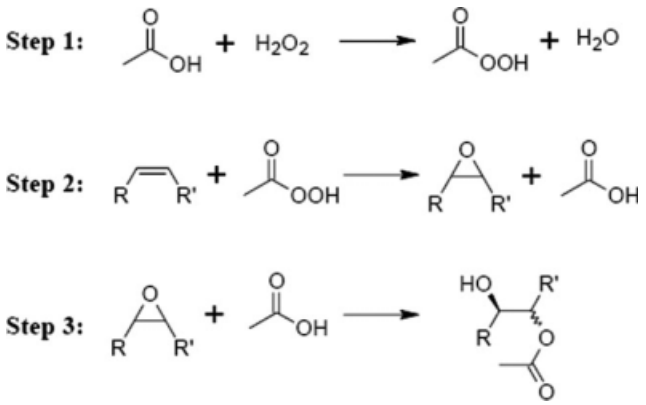

Scheme 2 Functionalization of soybean oil by epoxidation followed by hydroxylation.

surfactant (L-620), catalysts (D-19 and C-183), and deionized water were added to the polyols (ARCOL 3022 and Agrol-A) mixed at 3500 rpm for 60 s. The diisocyanate (TDI 80/20) was then added to the polyol and additive blends. The formulation blend was mixed at 3500 rpm for 10 s and immediately transferred to a wooden box lined with polyfilm, where it was allowed to rise. The foam was allowed to further cure overnight, under ambient conditions.

Foams based on Agrol-B SBP (Series B)

Foams samples were each synthesized in a 1000 mL popcorn cup, under ambient conditions. Initially, surfactant (DABCO DC198), catalysts (DABCO BL33LV and T12), and deionized water were added to the polyol and mixed at 2250 rpm for 15 s (VWR Power Max Elite Dual speed mixer). The diisocyanate was then added to the formulation (to obtain an isocyanate index of 1.1) and mixed at 2250 rpm for 10 s. The mixture was then allowed to rise and cure for 24 h, under ambient conditions.

Characterization techniques

Dynamic mechanical analysis (DMA)

Tests were performed on a Seiko DMS 210 tensile module with auto-cooler for precise temperature control. Rectangular foam samples ($12 \times 4 \times 2$ mm^3) were cut from the core of the foams and deformed along the blow direction (1 Hz frequency, 10 μm amplitude) in the tension mode, under a dry nitrogen atmosphere. The temperature was increased from -130 to 150°C, at a heating rate of 2°C/min.

Scanning electron microscopy (SEM)

Crushed foam samples were initially sputter coated with Au-Pd to a thickness of ca. 40 nm. The samples were then inserted in a Leo 1550 FESEM and micrographs were obtained at a working distance of ca. 26 mm and accelerating voltage of 20 kV. Images were obtained at a direction perpendicular to the blow direction.

Compression mechanical hysteresis. The mechanical hysteresis (MH) of the samples were measured using $30 \times 30 \times 30$ mm^3 foam samples in the compression mode on an Instron Model 4400 Universal Testing System controlled by Series IX software. Each sample was preconditioned by deforming it twice (perpendicular to the blow direction) to 75% of its initial thickness, at a rate of 240 mm/min, after which they were allowed to relax for 6 min, without any applied load. The samples were then cyclically compressed four times, to 75% of their initial thickness at 50 mm/min. Data was collected only during the last four cyclic deformation steps.

Indentation force deflection test. All the flexible foams were subjected to the indentation force deflection test (IFD) (ASTM D3574 95 B1) on the same INSTRON machine used in the MH test. Samples ($30 \times 30 \times 30$ mm^3) were preconditioned as mentioned earlier in the hysteresis test. The samples were compressed to 25% of its initial thickness at 50 mm/min and held in that deformed state for 1 min. The stress on the sample in this state (i.e., 25% deformation after 1 min) was reported as the 25% IFD value. The sample was then further compressed to 65% of the initial sample thickness and held in that deformed condition for 1 min (65% IFD). The sample was then unloaded to 25% of the initial thickness, held for 1 min (25% return IFD) and was then completely unloaded.

The support factor (SF) was calculated as the ratio of 65% IFD to 25% IFD.

Small angle X-ray scattering. Small-angle scattering (SAXS) measurements on the silica powders were performed using a Bonse-Hart camera covering a q-range of 0.0002–0.4 Å^{-1} (Beam line ID-33, Advanced Photon Source, Argonne National Laboratory, Argonne, IL). The X-ray beam was 0.4-mm high and 2-mm wide. To assist SAXS measurements, each foam sample was compressed between two aluminum plates to minimize void volume. The aluminum plates contained holes that were 1 cm in diameter for the X-ray beam to pass through. The foams, when compressed, had thicknesses that ranged from 4 to 6 mm. The data were corrected for sample transmission and for background scattering arising from air. The slit-smeared data were desmeared with Indra software (available on-line at www.uni.aps.anl.gov) and analyzed with Irena software, also available from Argonne National Laboratory.

RESULTS AND DISCUSSION

As stated earlier, two series of flexible PU foams were fabricated, where the PBP was increasingly

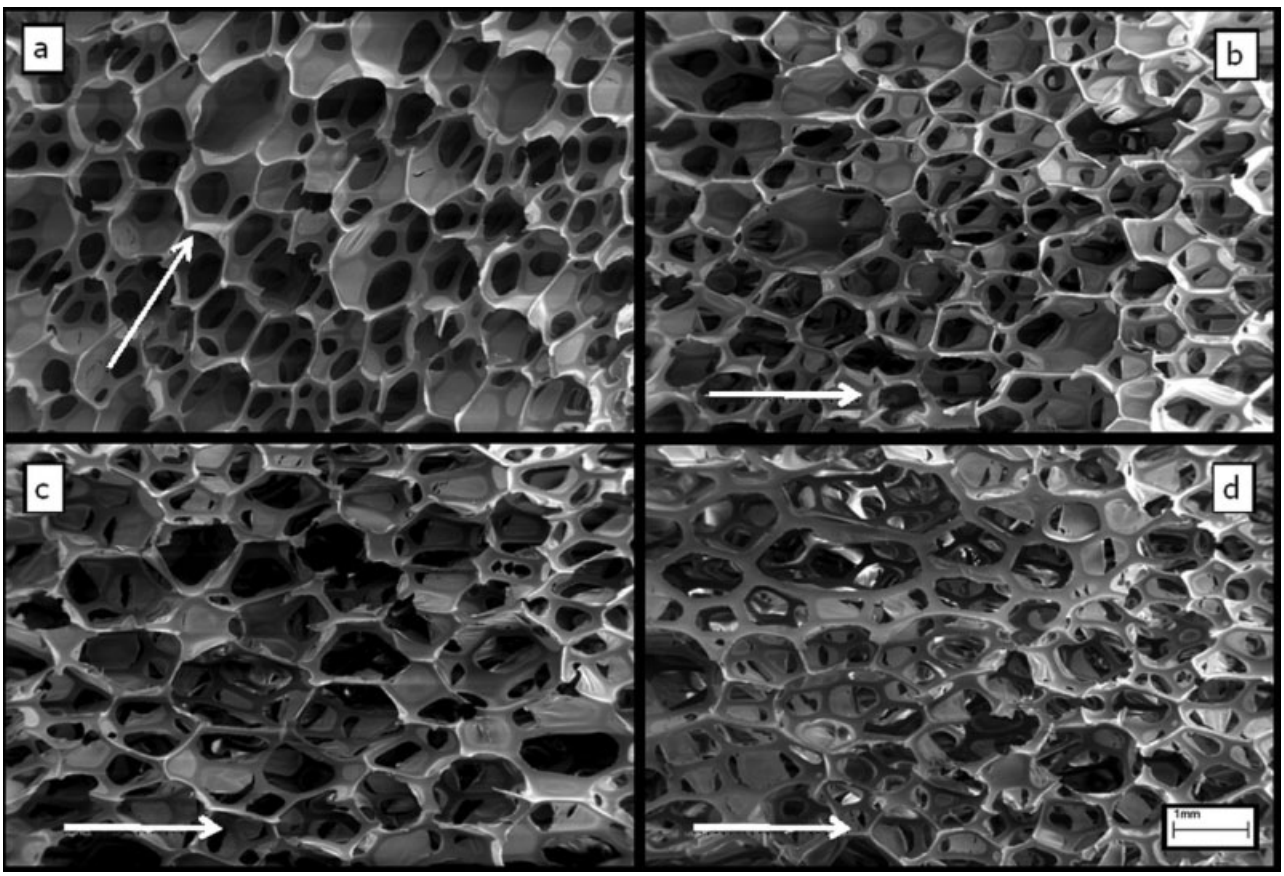

Figure 2 FESEM micrographs of Series A flexible PU foams containing various amounts of SBP Agrol-A: (a) 0, (b) 10, (c) 20, and (d) 30 wt % (scale bar denotes 1 mm). Blow direction shown by arrows.

replaced by SBP (Agrol-A in Series A and Agrol-B in Series B) in the foam formulation (0, 10, 20, 30 wt % relative to PBP), while keeping the relative ratio of the other ingredients (i.e., surfactant, water, and various catalysts) constant. Thus, this study would allow us to analyze the effect of SBP OH#, method of foam synthesis and incorporation of SBP, on the cellular morphology and mechanical properties of flexible PU foams.

The cellular morphology of the flexible PU foams was characterized by FESEM. All the foams studied, were mechanically crushed with our specially built, controlled crushing instrument to 75% of their original thickness (perpendicular to the blow direction) before analysis. This practice is common in specific segments of the foam industry and is performed to crush the foam cell windows, the excessive presence of which can lead to foam shrinkage and poor air flow-the latter greatly influences the utility of foams for cushioning. Results (Figs. 2 and 3) showed that though the cell size and strut size were similar for all the foams (Series A and B) analyzed, incorporation of SBP in the foam formulation always lead to an increased number of closed cells relative to the pure PBP-based foams, even after crushing. The number of closed cells was found to be slightly greater in Series B relative to the corresponding Series A foams [compare Figs. 2(d) and 3(d)], which may be attributed to the formation of a tighter urethane network structure in the former series, because of the higher OH# and functionality of the SBP utilized in Series B. Close inspection of the SEM micrographs revealed further differences in the cellular morphologies of the foams in Series A and B; e.g., whereas the cells in all the Series A foams were found to be asymmetrical in shape particularly when viewed perpendicular to their blow direction (shown by arrow) as expected (Fig. 2); the corresponding Series B foams were found to be more isotropic and also somewhat smaller in dimensions (Fig. 3). This lack of a strong anisotropy may be due to the fact that the Series B foams were fabricated in a much smaller scale and hence the cellular structure of these foams may have had a greater influence from the sides of the container, during the rise and cure of the foam.

The microphase separation behavior in the various flexible PU foams was analyzed by SAXS. All the flexible foams (Series A and B) showed the presence of a first order interference shoulder in their ambient SAXS profiles, confirming the presence of microphase separated morphology (Fig. 4). The

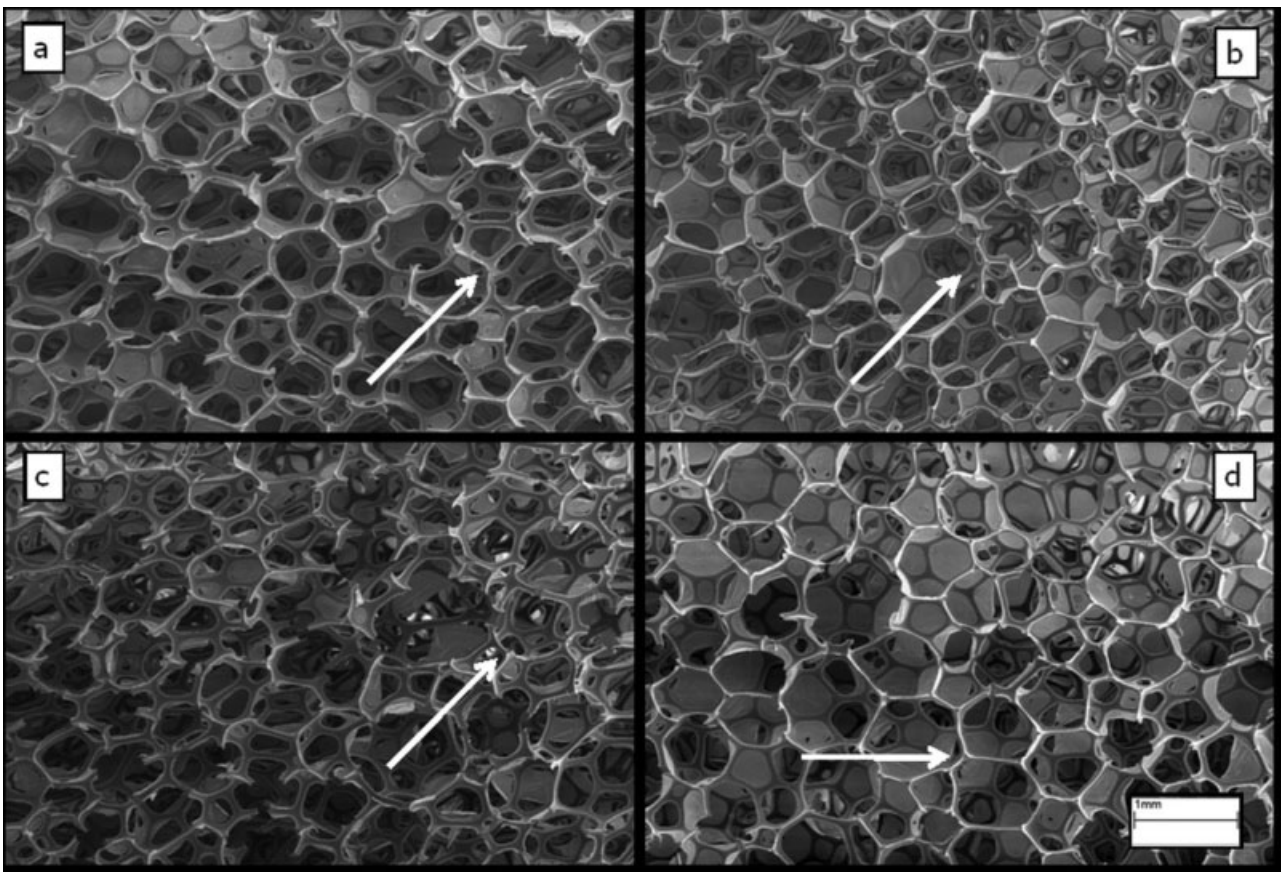

Figure 3 FESEM micrographs of Series B flexible foams based on various amounts of SBP, Agrol-B: (a) 0, (b) 10, (c) 20, and (d) 30 wt % (Scale bar represents 1 mm). Blow direction shown by arrows.

interdomain spacing (*d*-spacing) of the foams were found to be similar between the two Series analyzed (*d* of Series A and B were ca. 74 and 72 Å, respectively), suggesting that increasing the hydroxyl number of SBP (from 114 to 140) incorporated in the foam formulation and the foam fabrication procedure have only minor effects on the interdomain spacing of the microphase separated PU flexible foam. The SAXS profiles of the two series also showed only slight changes, as the fraction of SBP was increased in the foam formulations, e.g., the interference shoulder shifted very slightly to lower *q* in series A and the intensity profile became slightly broader in series B (the latter may suggest some

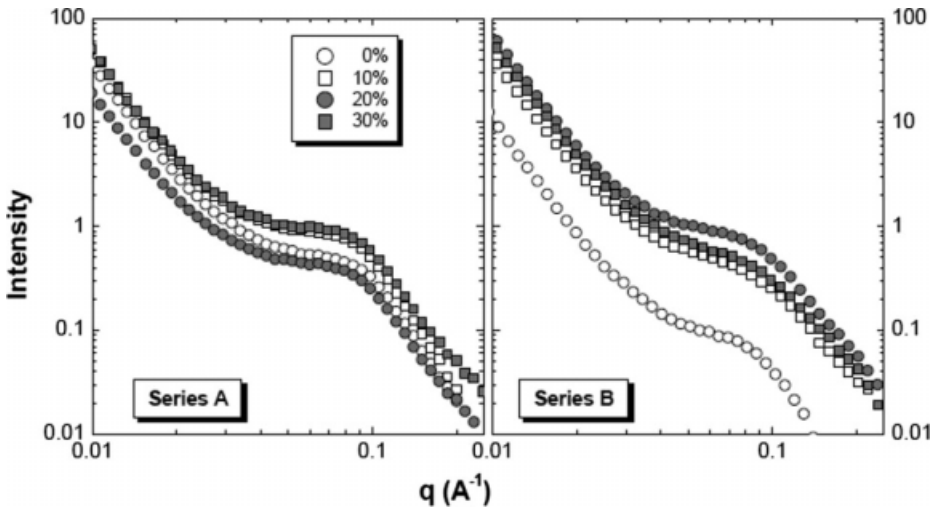

Figure 4 SAXS profiles of all the flexible PU foams investigated.

increased phase mixing, which was also indicated based on the DMA results as addressed below). The above-mentioned observations suggested, at best, only small changes in the microphase separated morphology of the flexible foams with the incorporation of SBP in the foam formulations.

The thermal behavior of the PU foams was analyzed by DMA. Like our past studies with flexible foams, the experimental modulus values were normalized to 3×10^9 Pa (in the range of polar, organic glassy polymers) at -130°C, which is well below the T_g of the elastomeric polyol. This was done because the samples were cellular in nature with void, air-filled regions, thereby making an accurate calculation of the true cross-sectional area of the sample difficult. The effect of incorporation of increasing amounts of SBP on the thermal transitional response of the foams can be visualized more clearly by analyzing the tan δ profiles because tan δ is the ratio of the loss modulus to storage modulus and thus the cross-sectional area of the samples cancel out. Hence, the tan δ transition features of a DMA plot are not influenced by foam density. Initially, the foams were characterized by DMA in both crushed and uncrushed forms. Our results showed that though the modulus of the uncrushed foams were slightly larger than the corresponding crushed foams (because of the presence of a relatively more closed cell structure in the uncrushed state), the thermal transition (observed with tan δ) was similar for both cases. Because we are interested in the thermal transitions of the PU foams, further DMA characterizations were conducted with uncrushed samples only. The thermal analysis was terminated at 150°C, because of the proximity of the degradation temperature (ca. 200°C) of flexible PU foams.

Figure 5 shows the DMA profiles of the various flexible PU foams in the temperature range of -130° to 150°C, in the uncrushed state. The DMA profiles of the various foams containing blends of PBP and SBP showed a single transition, which is attributed to the polyol T_g. As the SBP content in the foam formulations were increased, a significant and systematic change in the tan δ profiles of the flexible PU foams were observed in both the foam series:

- A systematic decrease in the tan δ intensity and systematic increase in the temperature of the polyol T_g, which may be attributed to the fact that a tighter network structure was formed as the PBP was increasingly replaced by the higher OH# and functionality SBP's.
- A systematic increase in the breadth of the tan δ response (which may possibly be attributed to the further phase mixing of the polyol and urea hard segments as was also suggested by the SAXS results).

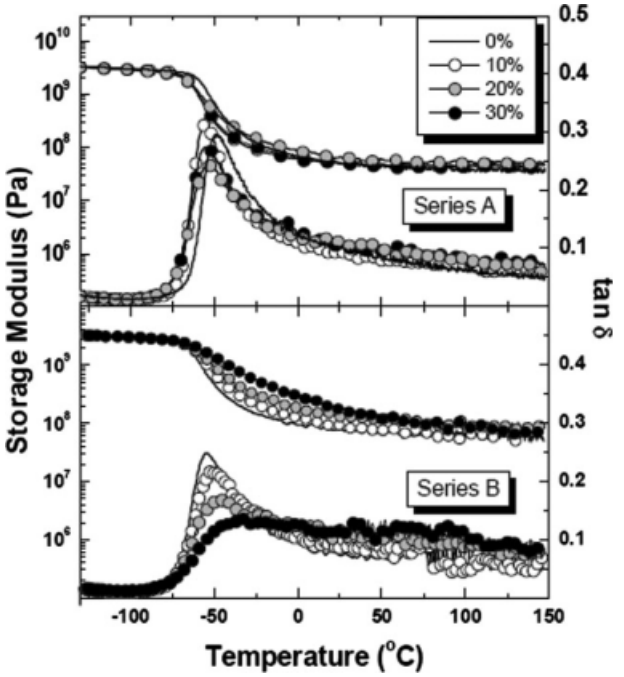

Figure 5 DMA profiles of all the flexible PU investigated.

Comparison of the DMA spectra between the two foam series studied showed that the effects of SBP incorporation (i.e., tan δ intensity decrease and urethane T_g increase) were found to be distinctly greater and more systematic in Series B foams (the SAXS results showed a slight increase in breadth of the intensity profiles in Series B only, with increased incorporation of SBP into the foam formulation, recall Fig. 4). The intensity of the tan δ peaks was found to be distinctly higher and the breadth of the mechanical relaxation was distinctly narrower in Series A foams relative to the Series B foams. Although the foam modulus at 25°C for Series B increased systematically with SBP incorporation, it showed very little change in the Series A foams; this affected the uniaxial stress–strain behavior of the flexible foams, as would be shown later in this report. Pechar et al.[34] extensively characterized the properties of PU elastomeric networks based on SBP's obtained from BBT and hydroxylated by the same methodology. He showed that the T_g of the networks cured with TDI had a linear relationship with the OH# of the SBP's, which was used to calculate the T_g of 100% SBP-based PU network (T_g's of 100% PU network based on Agrol-A and Agrol-B were ca. -14° and 17°C, respectively). Though the formulation and cure process of those particular elastomeric PU networks (cured at 100°C for 3 h) and the flexible PU foams (cured under ambient conditions, overnight) are different, the relationship between the polyol T_g and polyol hydroxyl number should have similar

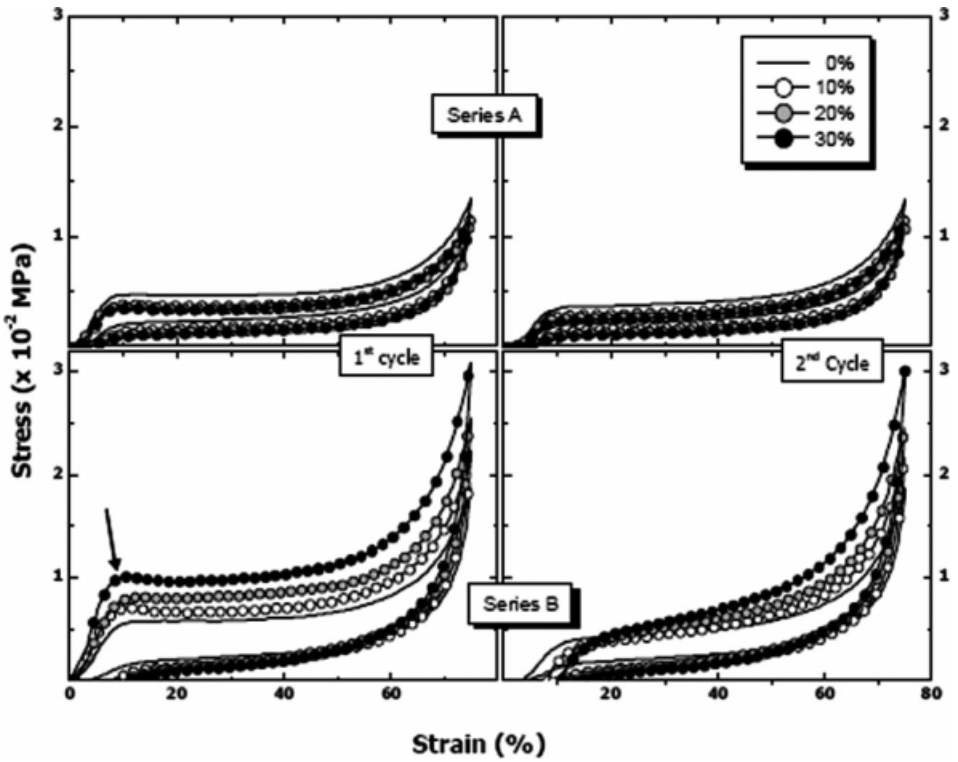

Figure 6 Mechanical hysteresis behavior measured in a compression mode for all the flexible PU foams investigated.

trends in both systems. Thus, the relatively greater SBP effects observed in Series B may be attributed to the incorporation of the higher T_g SBP which also leads to the formation of a relatively tighter network than the corresponding Series A foams.

The mechanical hysteresis (MH) is a measure of the amount of energy dissipated per cycle by flexible foams when cyclically deformed and gives one measure of the durability and vibrational damping ability of the foams. MH of all the foams was measured in the compression mode under ambient conditions. As stated earlier, the preconditioned samples were cyclically compressed four times, to 75% of their initial thickness at 50 mm/min. The 1st and 2nd hysteresis cycles were found to be different (Fig. 6), whereas the latter cycles (i.e., 3rd and 4th cycles) were found to be similar to the 2nd cycle in all cases as expected. Results showed that incorporation of SBP into the foam formulation led to a systematic increase in MH in both foam Series (Table II). But several significant differences in the MH behavior were observed between the two foam series.

- The stress on foams from Series A was found to be lower than the corresponding foams from Series B under all conditions.
- Although the stress on the samples at 75% strain was found to decrease slightly in Series A foams with incorporation of SBP, it was found to increase systematically in the corresponding

TABLE II
Effect of Replacing PBP with SBP on the Mechanical Hysteresis Behavior of all the Flexible PU Foams Investigated

SBP type	SBP content (wt %)	Hysteresis (%)[a] Cycle 1	Hysteresis (%)[a] Cycle 2	Stress at 75% strain[a] ($\times 10^{-2}$ MPa)
Agrol-A	0	41 ± 1	33 ± 1	1.28
	10	46 ± 1	39 ± 1	1.13
	20	49 ± 1	41 ± 1	1.08
	30	52 ± 1	44 ± 1	1.19
Agrol-B	0	54 ± 3	45 ± 2	1.84
	10	59 ± 2	48 ± 3	1.72
	20	63 ± 1	52 ± 1	2.56
	30	70 ± 1	58 ± 2	3.11

[a] Average of three replications.

foams from Series B, under similar circumstances (Table II).

- A distinct necking behavior was observed in the 1st hysteresis cycle for the 30% SBP-based foam from Series B, but this behavior was absent in all the other SBP-based foams (both Series A and B).
- Although the instantaneous set (described as the strain remaining on the sample at zero stress in their 1st unloading cycle) of foams from Series A were similar, it was found to increase systematically with incorporation of Agrol-B SBP in Series B.

The differences indicated above are strongly believed to be due to some differences in cell anisotropy and particularly the OH# differences between the two foam series, the latter led to the formation of a tighter urethane network structure with more closed cells and/or slightly better phase mixing in Series B relative to the corresponding foams from Series A. The modulii of the flexible foams (the slope of the initial linear part of the stress-strain curves) were also found to be different in the two series studied; it was found to decrease slightly in Series A (note the slight decrease in the slope of the initial part of the stress-strain curve with SBP content), but was found to increase systematically in Series B (systematic increase in the initial stress-strain slope with SBP content). This trend is also directly supported by the differences in the ambient storage modulus of the flexible foams (recall the respective DMA curves in Fig. 5) in the two series brought about by formation of a tighter network structure in Series B compared to Series A.

The IFD test, which is widely used to measure the firmness and load-bearing capability of flexible PU foams, was performed on all foam samples following the ASTM D3574 95 B1 procedure (Fig. 7). The PBP foams in both series had similar IFD-values. But while all the IFD-values (i.e., 25% IFD, 65% IFD, and 25% return IFD) decreased systematically with incorporation of SBP in Series A, they were found to increase in the corresponding Series B. This may be attributed to the presence of a relatively larger number of closed cells in the Series B foams.

The support factor (SF, which is defined as the ratio of 65% IFD to 25% IFD) denotes the ability of a flexible foam to support force at different indentation levels. It is found to be affected by the foam density and foam formulation and manufacturing process. The SF of conventional foams range between ca. 1.8 and 3.0. Our result showed (Fig. 7) that the SF increase slightly but systematically with the incorporation of the SBP in Series A foams, but did not change appreciably in the corresponding Series B foams. As the density of all the flexible foams in either series were similar to each other, the above-

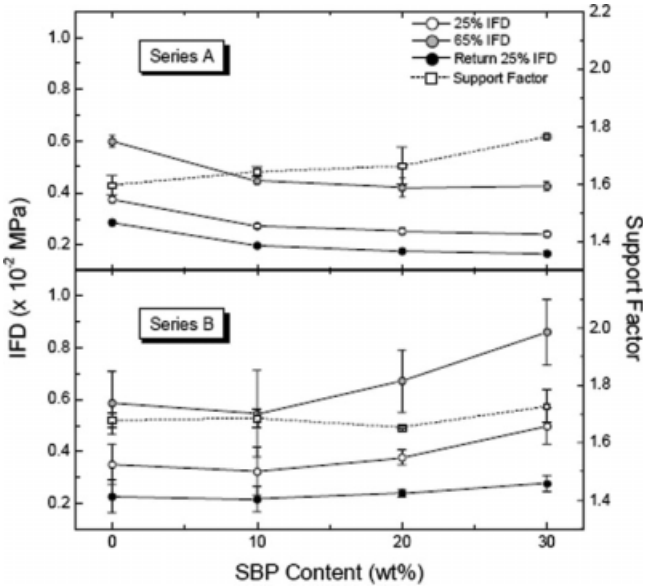

Figure 7 IFD-values and support factors of all the flexible PU foams investigated (measured in compression mode).

mentioned differences may be attributed to the different fabrication process and/or different polyol OH#s, utilized in manufacturing the two foam series, which led to the formation of foams with somewhat different cellular structures and cell anisotropy, as was confirmed by the SEM analysis (Figs. 2 and 3). We attribute the systematic increase in the SF of Series A foams to be due to the increase in cell anisotropy and the larger number of closed cells with the incorporation of SBP.

CONCLUSIONS

This study was undertaken to probe how the cellular morphology and mechanical properties of flexible PU foams were affected by the substitution of conventional PBP with SBP in a flexible foam formulation. The hydroxyl number of the SBP and the foam fabrication process were also varied to see their effects on the above-mentioned properties of the flexible foams. Our results showed that the foam composition and their fabrication process had a significant effect on the cellular morphology and anisotropy of the flexible foams. All the foams were microphase separated and the SAXS "*d*"-spacings changed only slightly as the OH# of the incorporated SBP was increased. The polyol T_g was found to systematically broaden, shift to slightly higher temperatures and the number of closed cell windows in the cellular structure of the PU foam increased with incorporation of the SBP into the foam formulation; these affects were found to be relatively greater in the flexible foams synthesized with the SBP with higher OH# which formed a relatively tighter network structure than the corresponding

lower OH# SBP analogue. The mechanical properties of the flexible foams were also found to change systematically with incorporation of the SBP. Thus, our results clearly show that SBP can be utilized to produce foams possessing respectable properties.

The authors would like to thank Dow Chemical Company for donating the petro-based polyol and Air Products for donating the various surfactants and catalysts that were used in this study. The authors would also like to acknowledge D. Kohls and Dr. D.W. Schaefer, Department of Chemical and Mechanical Engineering, University of Cincinnati, for performing the USAXS measurements on all the flexible foam samples.

References

1. Bayer, O. Angew Chem 1947, 59, 257.
2. Herrington, R. In Flexible Polyurethane Foams; Herrington, R.; Hock, K., Eds.; The Dow Chem Company, 1997.
3. Wirpsza, Z. Polyurethanes: Chemistry, Technology and Applications; Ellis Horwood: New York, 1993.
4. Wilkes, G. L.; Abouzahr, S.; Radovich, D. J Cell Plast 1983, 19, 248.
5. Armistead, J. P.; Wilkes, G. L. J Appl Polym Sci 1988, 35, 601.
6. Elwell, M. J.; Mortimer, S.; Ryan, A. J. Macromolecules 1994, 27, 5428.
7. Elwell, M. J.; Ryan, A. J.; Grunbauer, H. J. M.; Lieshout, H. C. V. Macromolecules 1996, 29, 2960.
8. McClusky, J. V.; Priester, R. D. J.; O'Neill, R. E.; Willkomm, W. R.; Heaney, M. D.; Capel, M. A. J Cell Plast 1994, 30, 338.
9. Dounis, D. V.; Wilkes, G. L. J Appl Polym Sci 1997, 66, 2395.
10. Dounis, D. V.; Wilkes, G. L. Polymer 1997, 38, 2819.
11. Kaushiva, B. D.; Dounis, D. V.; Wilkes, G. L. J Appl Polym Sci 2000, 78, 766.
12. Kaushiva, B. D.; McCartney, S. R.; Rossmy, G. R.; Wilkes, G. L. Polymer 1999, 41, 285.
13. Moreland, J. C.; Wilkes, G. L.; Turner, R. B. J Appl Polym Sci 1994, 52, 549.
14. Moreland, J. C.; Wilkes, G. L.; Turner, R. B. J Appl Polym Sci 1994, 52, 569.
15. Hoefer, R.; Daute, P.; Grutzmacher, R.; Westfechtel, A. J Coating Technol 1997, 69, 65.
16. Lyon, C. K.; Garrett, V. H.; Frankel, E. N. J Am Oil Chem Soc 1974, 51, 331.
17. Reed, D. Ureth Technol 1997, 14, 20.
18. Hu, Y. H.; Gao, Y.; Wang, D. N.; Hu, C. P.; Zu, S.; Vanoverloop, L.; Randall, D. J Appl Polym Sci 2002, 84, 591.
19. Javni, I.; Petrovi, Z. S.; Guo, A.; Fuller, R. J Appl Polym Sci 2000, 77, 1723.
20. Evans, C. D.; List, G. R.; Beal, R. E. J Am Oil Chem Soc 1974, 51, 444.
21. Khot, S. N.; Lascala, J. J.; Can, E.; Morye, S. S.; Williams, G. I.; Palmese, G. R.; Kusefoglu, S. H.; Wool, R. P. J Appl Polym Sci 2001, 82, 703.
22. John, J.; Bhattacharya, M.; Turner, R. B. J Appl Polym Sci 2002, 86, 3097.
23. Liu, K. Soybeans: Chemistry, Technology and Utilization; Chapman & Hall: New York, 1997.
24. Gao, A.; Javni, I.; Petrovi, Z. S. J Appl Polym Sci 2000, 77, 467.
25. Uyama, H.; Kuwabara, M.; Tsujimota, T.; Nakano, M.; Usuki, A.; Kobayashi, S. Chem Mater 2003, 15, 249.
26. Gao, A.; Cho, Y.; Petrovi, Z. S. J Polym Sci Part A: Polym Chem 2000, 38, 3900.
27. Kandanarachchi, P.; Gao, A.; Petrovi, Z. S. J Mol Catal A Chem 2002, 184, 65.
28. Guo, A.; Zhang, W.; Petrovic, Z. J Mater Sci 2006, 41, 4914.
29. Singh, A. P.; Bhattacharya, M. Polym Eng Sci 2004, 1977, 44.
30. Mielewski, D. F.; Flanigan, C. M.; Perry, C.; Zaluzec, M. J.; Killgoar, P. C. Ind Biotechnol 2005, 1, 32.
31. Herrington, R.; Malsam, J. U.S. Pat 2005/0070620, 2005.
32. Zhang, L.; Jeon, H. K.; Malsam, J.; Herrington, R.; Macosko, C. W. Polymer 2007, 48, 6656.
33. Casper, D. M.; Newbold, T. U.S. Pat. 20,060,041,156, 2006.
34. Pechar, T. W.; Wilkes, G. L.; Zhou, B.; Luo, N. J Appl Polym Sci 2007, 106, 2350.